Jianzhe Huang, Associated Professor Department of Power and Energy Engineering Harbin Engineering University, Harbin, China

David A. Peters, McDonnell Douglas Professor of Engineering Department of Mechanical Engineering & Materials Science Washington University in St. Louis, St. Louis, USA

Abstract

The finite-state inflow model is widely used in real-time simulations. Coupling such a model with rotor blade flapping requires that the induced velocity be computed at the rotor disk, but the model also allows the flow to be computed at any location in the flow field above the rotor plane. However, to compute the flow field below the rotor disk (such as is required for co-axial rotors) requires computation of the adjoint variables (along with the normal state variables) including a time delay. Since the adjoint variables must be marched backwards in time, this can pose a problem in real time analysis. In this paper, computation of the adjoint variables (and flow below the disk) is addressed in the time domain. For illustrative purposes, the parameters for the two-blade Harrington coaxial rotor are used. A step input is given to collective pitch in hover. The blade sectional lift is then calculated based on combined blade-element theory and on dynamic wake modeling (including blade flapping). These equations are first time-marched forward to give the conventional state variables in the time domain. The co-state theorem is then introduced to calculate the co-states and the induced velocity below the rotor. Two alternatives methods are explored in order to compute the adjoint variables with time-delay. The first is the convolution method (in which at every time steps the adjoint variables are computed by a closed-form convolution). The second method is to march backwards in time for the co-states (i.e., adjoint variables). Two methods are considered for this second method: 1.) time marching backwards at every three time steps, and 2.) time-marching backwards once at the end of the domain of interest. The various methods are compared for computational efficiency and numerical accuracy.

1. Background

Pitt and Peters [1] offered a finite-state induced flow theory based on the potential-flow equations. The model could have from three to five inflow states. Peters and He [2] generalized the method to an arbitrary number of states by the use of superposition of pressures, giving the normal component of flow on the disk. Peters and Cao [3] tried to extend the model to flow off the disk, but were unsuccessful. However, they did demonstrate that a second set of inflow states would be necessary for flow off the disk. Morillo and Peters [4] found the extra states for flow above the disk, but were unable to find the singular members of the set—thus yielding poor convergence. Yu and Peters [5] were able to improve convergence but still could not find the singular states. Hsieh, Duffy, and Peters [6] finally found the singular states and were able to find flow off the disk but not in the wake. Fei and Peters [7] showed that flow within the wake also required the solution of adjoint variables. Huang [8] successfully applied the adjoint theorem to find all components of induced flow everywhere in the disk in the frequency domain. However, to compute the velocity below the disk, it requires the

adjoint velocity on the disk with time-delay. To get such a velocity, it requires to time-marching the equations backward which could be time-consuming when the states increase. For real time simulation, the speed of the computation is of great importance. Hence, it is necessary to seek a more effective way to achieve a fast and accurate computation of the adjoint variable with time delay.

In this paper, the dimensional finite state inflow model will be solved numerically in the time domain coupling with dynamics of blade flapping through simpletic method. The co-states theory will be applied to give the solution of the induced velocity below the disk. The convolution method to calculate the adjoint variables will be introduced as well as the other two methods which are to march backwards in time for the co-states with different approaches. The simulation results will be discussed to show that the convolution approach is practical for real-time simulations.

2. Method descriptions

For a lifting rotor in hover, the rotation speed and the free-stream are assumed to be Ω and V_{∞} , respectively. Then the finite-state inflow model for such a rotor in hover condition can be given in Eq. (1), and the state variables can be obtained numerically with specific initial conditions.

$$R[M]\{a_n^m\}+[D][V][L]^{-1}[M]\{a_n^m\}=[D]\{\tau_n^m\}$$
 (1) where R is the radius of the rotor; $[M]$ is apparent mass matrix; $[D]$ is the damping matrix; $[L]$ is the influent coefficient matrix. The matrix $[V]$ is defined as

$$\begin{bmatrix} V \end{bmatrix} \triangleq \begin{bmatrix} V_T & & & \\ & V & & \\ & & \ddots & \\ & & & V \end{bmatrix}$$
 (2)

where

$$V_T = V_{\infty} + v_{ave}$$

$$V = \frac{\left(V_{\infty} + v_{ave}\right)\left(V_{\infty} + 2v_{ave}\right)}{V_{T}}$$

$$v_{ave} = \frac{2}{\sqrt{3}} \{1 \quad 0 \quad \cdots \quad 0\} [L]^{-1} [M] \{a_n^m\}$$

$$V_{\infty} = \Omega R \eta$$

 v_{ave} is the average induced velocity within the rotor disk region and η is the climb rate. The input $\left\{\tau_n^m\right\}$ can be calculated using Eq. (3).

For
$$n = 1, 3, ...,$$

$$\tau_n^0 = \frac{1}{2\pi} \sum_{q=1}^{Q} \int_0^1 \frac{L_q}{2\rho R} J_0(0) \phi_n^0(r) dr;$$
For $m = 1, 2, ...$ and $n = m+1, m+3, ...,$

$$\tau_n^m = \frac{1}{\pi} \sum_{q=1}^{Q} \int_0^1 \frac{L_q}{2\rho R} J_0(m\overline{b}/r) \phi_n^0(r) dr \cos(m\psi_q);$$
Others, $\tau_n^m = 0$.

where ρ is air density, Q is number of blades, r is normalized length from the root of the blade to the point to compute and r = x/R, ψ_q is azimuth angle of the q^{th} blade and $\psi_q = \Omega t + 2\pi/Q \ (q-1)$, \bar{b} is the non-dimensional semi-chord and $\bar{b} = c/2R$. $\phi_n^0(r)$ can be expressed in terms of the Legendre function of the first kind in the ellipsoidal coordinate system.

$$\phi_n^m(r) = \frac{1}{\nu} P(\nu) \tag{4}$$

The ellipsoidal coordinate system (v, η, ψ) can be transformed from the rectangular coordinates as

$$v = \frac{-sign(z)}{\sqrt{2}} \sqrt{1 - \overline{S} + \sqrt{(\overline{S} - 1)^2 + 4z^2}},$$

$$\eta = \frac{1}{\sqrt{2}} \sqrt{\overline{S} - 1 + \sqrt{(\overline{S} - 1)^2 + 4z^2}},$$

$$\psi = \tan^{-1} \left(\frac{-y}{x}\right),$$

$$\overline{S} = x^2 + y^2 + z^2.$$
(5)

The sectional lift per unit length for the qth blade for lifting rotor in hover can be obtained through the combined blade element theory as

$$L_{q} = \frac{1}{2} \rho ac \left[\Omega^{2} x^{2} \theta - \Omega x \left(V_{\infty} + v + \dot{\beta}_{q} x \right) \right]$$
 (6)

where a is the slope of the lift coefficient C_L , β_q is the angle of flapping for the q^{th} blade. The induced velocity for the center point of the blade element at time t can be written in Eq. (7).

$$v = \sum_{m=0}^{\infty} \sum_{n=m}^{\infty} a_n^m P_n^m(v) Q_n^m(i\eta) \cos(m\psi_q)$$
 (7)

For the induced velocity on the rotor disk, $\eta = 0$ and $Q_n^m(i\eta) = 1$. θ is the pitch angle which is given as

$$\theta = \theta_0 + \theta_c \cos \psi_a + \theta_s \sin \psi_a \tag{8}$$

where θ_0 is the collective pitch, θ_c and θ_s are the cyclic pitch.

The equation of motion of the q^{th} blade is

$$I_{y}\ddot{\beta}_{q} + \left(\Omega^{2}I_{y} + K_{\beta}\right)\beta_{q} = \int_{0}^{R} L_{q}xdx \tag{9}$$

where I_y and K_β are the moment of inertia and elastic coefficient of the root spring for the q^{th} blade, respectively. March Eqs. (1) and (9) in time with initial conditions using the method of simpletic, the state variables can be computed.

For induced velocity below the rotor disk, the Adjoint velocity should be computed. The adjoint equations can be given as

$$-\left\{\Delta_{n}^{m}\right\}+\left[A\right]\left\{\Delta_{n}^{m}\right\}=\left[B\right]\left\{\tau_{n}^{m}\right\} \tag{12}$$

where

$$[A] = R^{-1}[M]^{-1}[D][V][L]^{-1}[M]$$
$$[B] = R^{-1}[M]^{-1}[D]^{-1}(-1)^{n+1}$$

The eigenvalues $\{\eta_i\}$ and eigenvector $[\varphi]$ of matrix [A] has the following relationship

$$[\varphi]^{-1}[A][\varphi] = \begin{bmatrix} \eta_1 & & \\ & \ddots & \\ & & \eta_i \end{bmatrix}$$
 (13)

The closed-form solution of adjoint variables with time delay ζ is given as

$$\left\{ \Delta_n^m(t - \varsigma) \right\} = \int_{t - \varsigma}^t \left[\varphi \right] \left[W \right] \left[\varphi \right]^{-1} \left[B \right] \left\{ \tau_n^m(\alpha) \right\} d\alpha \quad (14)$$

where

$$[W] = \begin{bmatrix} e^{-\eta_1(\alpha - t + \varsigma)} & & & \\ & \ddots & & \\ & & e^{-\eta_1(\alpha - t + \varsigma)} \end{bmatrix}$$

Based on Eq. (14), the adjoint variables can be calculated numerically which is called as method 1.

In [8], the induced velocity below the disk can be obtained as

$$v(x, y, z, t) = v(z, r, \psi, t)$$

$$= v(0, r_0, \psi_0, t - \xi)$$

$$+ v^*(0, r_0, \psi_0 + \pi, t - \xi)$$

$$- v^*(-z, r_0, \psi_0 + \pi, t)$$
(15)

where $\xi = z/V_{\infty}$ and the adjoint velocity is calculated as

$$v^* = \sum_{m=0}^{\infty} \sum_{n=m}^{\infty} \Delta_n^m P_n^m(v) Q_n^m(i\eta) \cos(m\psi)$$
 (16)

The convolution method, in Eq. (14), can be used to find the adjoint variables. The third term in Eq. (15) is 0 because, by definition the adjoint variables are 0 when $t = \tau$. As an alternative to the application of the convolution method, the adjoint variables can also be obtained through marching Eq. (12) backward in time with algorithm of sempletic. There are two approaches to this. One is to march Eq. (12) backward in time with zero initial conditions from the end time of the computational period (method 2). For method 3, the adjoint variables are updated every three time steps by marching Eq. (12) backward while the induced velocity is computed in time.

3. Results

For the Harrington rotor, the system parameters are given in Eq. (17). In the hover conditions of such a rotor, the climb rate is assumed to be 0.12.

$$R = 12.5 \text{ ft}, c = 1.5 \text{ ft}, \Omega R = 262 \text{ ft/s}, a = 4.3,$$

 $Q = 2, I_{\beta} = 1765 \text{ slug} \cdot \text{ft}^2, K_{\beta} = 4000 \text{ ft} \cdot \text{lb/rad.}$ (17)

Based on the momentum theory, the coefficient of the thrust in hover can be obtained as

$$C_T = \frac{2v_{ave}(v_{ave} + V_{\infty})}{(\Omega R)^2}$$
 (18)

For the ratio of the rotor thrust coefficient to the solidity is assume to be 0.08, the average induced velocity on the rotor disk can be obtained. Then the control schemes can be further determined as

$$\theta_0 = \frac{6C_T}{\sigma a} + \frac{2}{3} \frac{v_{ave} + V_{\infty}}{\Omega R}, \theta_c = \theta_s = 0$$
 (19)

For the step input, only τ_1^0 will be considered in such a finite-state inflow model and Eq. (7) can be simplified as

$$v = a_1^0 P_1^0(v) Q_1^0(i\eta)$$
 (20)

With the parameters of Eq. (17), the induced velocity due to a step input is computed, Fig.1. The step response peaks at about 234 ft²/s², and oscillates for several seconds reaching 181 ft²/s². Results at x = -0.8R, y = 0, z = 1.2R in the hover are presented in Figs. 2-4 for methods 1-3, respectively. For the climb rate of 0.12 in hover, the free-stream velocity is 31.44 ft/s. For the induced velocity 1.2 radii below the disk, the time delay for the adjoint variable will be 0.477 s. Therefore, to compute the velocity in the range of $t \in [0,10]$, adjoint variable are required for $-0.477s \le t \le 9.523s$ according to Eq. (15). It can be found that the adjoint variable and induced velocity reach steady state faster than the step input. For the induced velocity, method 1 and method 3 give almost the same result at the steady states. The steady state velocity for method 2 has approximate 8% difference compared with value for the other two methods. Additionally, method 2 gives a small artificial dip in velocity in the interval $9.5s \le t \le 10s$, which is illustrated in Fig. 3(b). Although in theory the final result of the last two terms in the adjoint theorem which is given in Eq. (15) is independent of initial conditions on $\Delta_1^0(t)$, in practice there will be a slight difference in this value due to initial conditions if an infinite number of modes are not included. Because $\Delta_1^0(t)$ varies so rapidly in the interval $9.5s \le t \le 10s$ which is shown in Fig. 3(a), the error for such a value is as large as it would ever get, which is about 2.2%. Although such an error is not large, it does show that there is some residual due to truncation of states. For the method 3 which is shown in Fig. 4, though it can get similar result as method 1, the computation effort will be greatly increased compared to method 2.

This comparison shows that the convolution method is numerically more robust than time marching backwards all the way from t=10, and the computation time for such a method can be obviously reduced compared with method 3. The added robustness is due to the fact that the convolution method continually re-initializes on zero initial conditions $v^*(t) = 0$ at every time step, and thus error can be minimized.

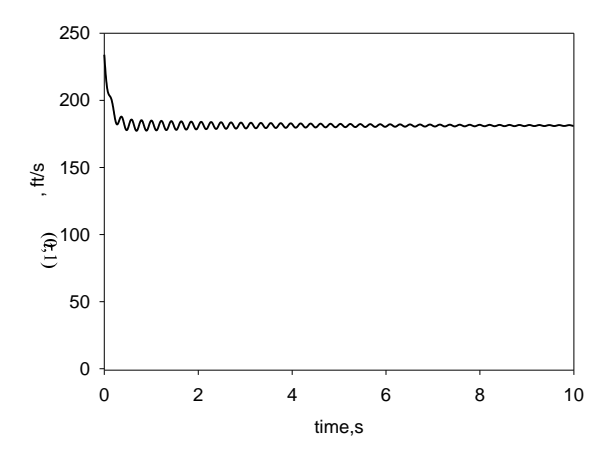
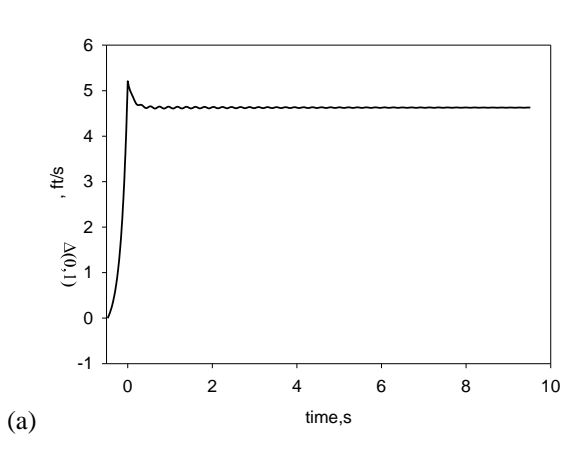


Fig. 1 Step input τ_1^0 in the hover condition.



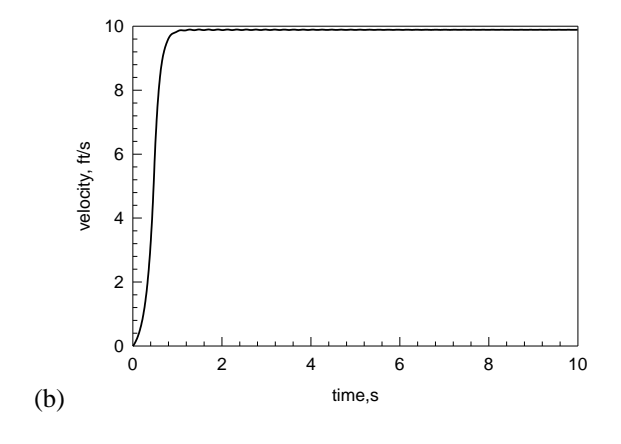
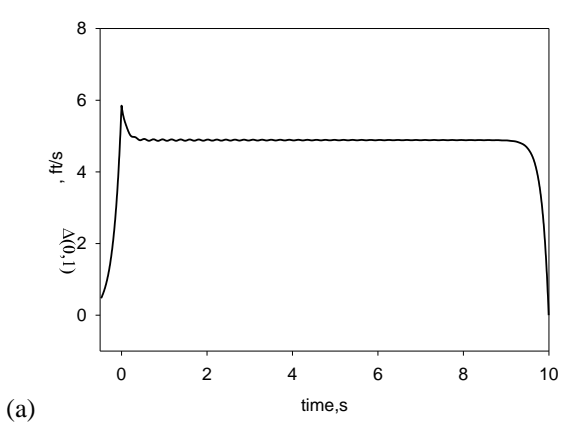


Fig. 2 Computation results for x = 0.8R, y = 0.0, z = 1.2R with step input in the hover condition through method 1: (a) Adjoint variable Δ_1^0 and (b) induced velocity.



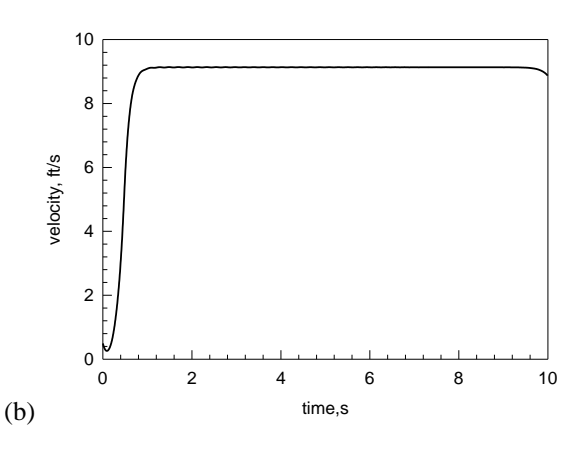


Fig. 3 Computation results for x = 0.8R, y = 0.0, z = 1.2R with step input in the hover condition through method 2: (a) Adjoint variable Δ_1^0 and (b) induced velocity.

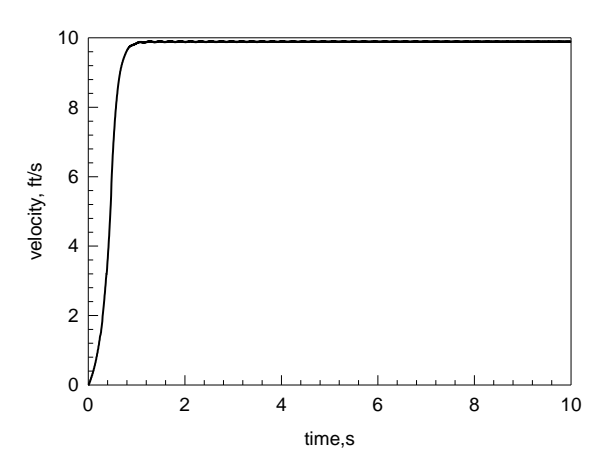


Fig. 4 Induced velocity for x = 0.8R, y = 0.0, z = 1.2R with step input in the hover condition through method 3.

To achieve higher accuracy of computation, sufficient states should be included [9]. Herein, 6

harmonics for odd terms and 5 harmonics for even terms will be adopted for the solution and totally 15 states will be involved. In Fig.5, the induced velocity at x = 0.8R and y = 0.0 on the rotor disk is illustrated. The velocity is approaching steady-state after 0.4 seconds. Within one period of rotation which is about 0.3 seconds, the induced velocity reaches the peak value twice since the blade number is two. The average value of the induced velocity at such location after steady-state is about 9.55 ft/s. The induced velocities at 0.2R, 0.8R, 1.2R below the disk are demonstrated in Figs. 6-8, respectively. The average induced velocity increases quickly from 15.15 ft/s to 18.67 ft/s, which is about twice as the average induced velocity at the rotor disk. It can also be observed that the induced velocity start to oscillate later as it moves more away from the rotor disk plane.

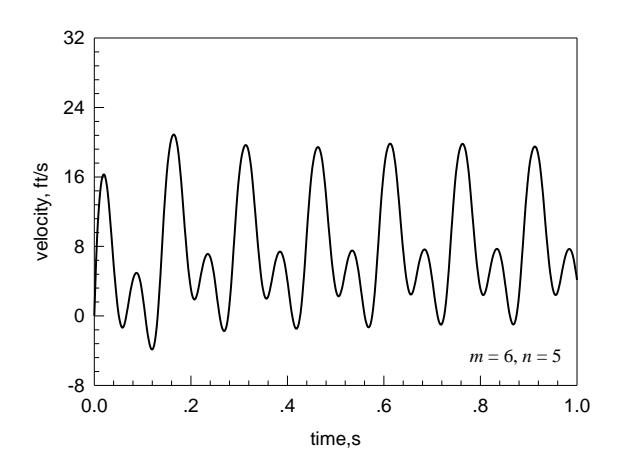


Fig. 5 Induced velocity for x = 0.8R, y = 0.0, z = 0.0 with 15 states in the hover condition.

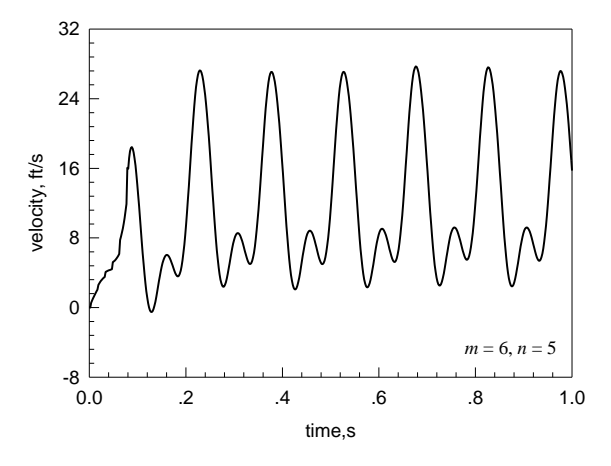


Fig. 6 Induced velocity for x = 0.8R, y = 0.0, z = 0.2 with 15 states in the hover condition through method 1.

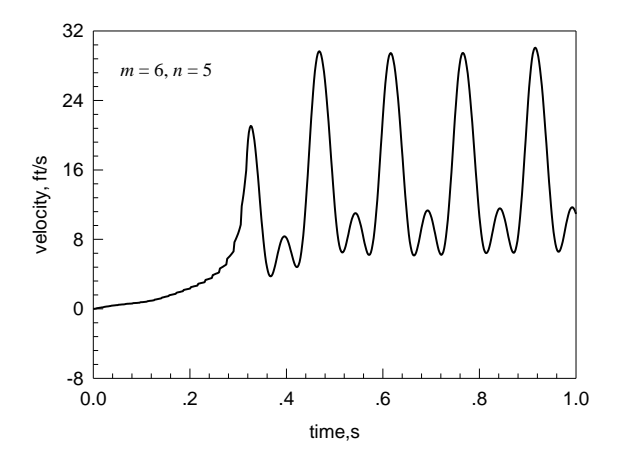


Fig. 7 Induced velocity for x = 0.8R, y = 0.0, z = 0.8 with 15 states in the hover condition through method 1.

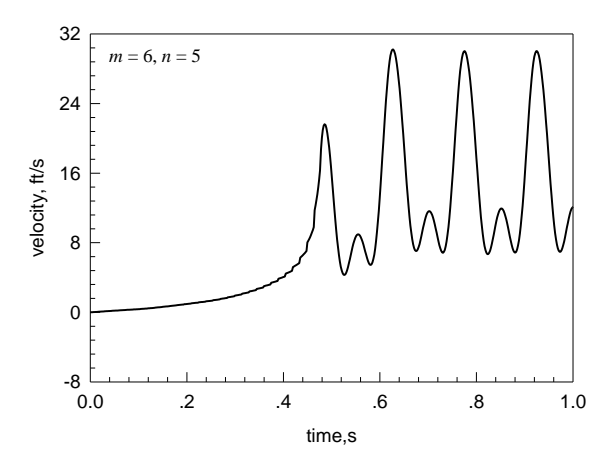


Fig. 8 Induced velocity for x = 0.8R, y = 0.0, z = 1.2 with 15 states in the hover condition through method 1.

With such a convolution approach, the induced velocity contours 0.4 radii and 0.8 radii below the disk in hover condition computed using the 15 states finite state inflow model are presented in Figs.9 and 10, respectively. The computational time is 1 second, and x is in the range of [-2.0R, 2.0R]. From both of the plots, it can be seen that the induced velocity is very low at the centerline of the rotor, and the velocity gradient is very high around $x = \pm R$.

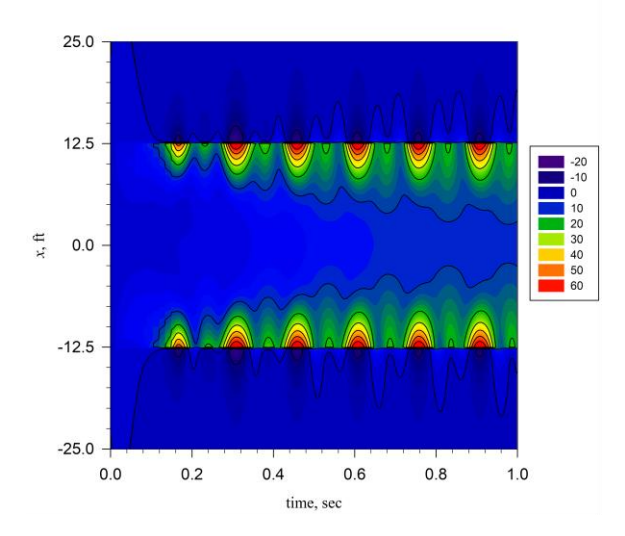


Fig. 9 Induced velocity contour for y = 0, z = 0.4R with 15 states in the hover condition through method 1

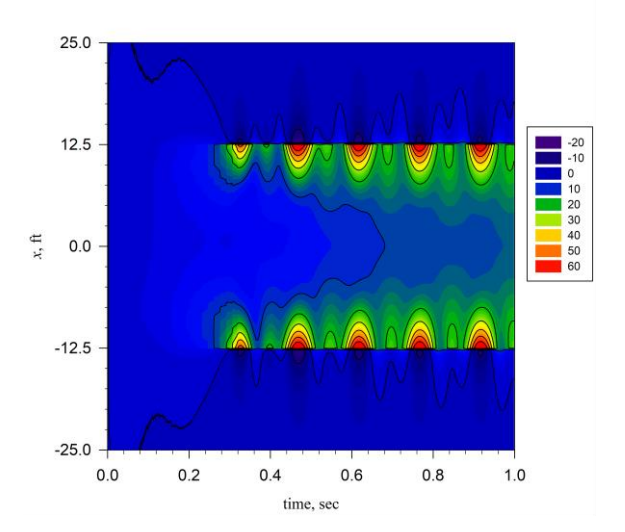


Fig. 10 Induced velocity contour for y = 0, z = 0.8R with 15 states in the hover condition through method 1.

4. Conclusions

It is demonstrated that three different methods can be used for computation of the adjoint variables in the time domain, leading to identical responses for flow below the disk. The method that employs the convolution integral is the most efficient and holds promise in solutions of adjoint variables in real time. The induced velocities in hover at different locations below the disk based on the 15-state model have been discussed, and the magnitude increases when it goes deeper into the wake. The induced velocity contours

have also been obtained to show how the velocity distributes on and outside of the rotor disk region.

Acknowledgement

This work was sponsored by the Rotorcraft Centers of Excellence through the Georgia Tech/Washington University Center of Excellence, Dr. Mahendra Bhagwat, technical monitor.

References

- [1] Pitt, Dale. M. and Peters, David A., "Theoretical Prediction of Dynamic-Inflow Derivatives," Vertica, Vol. 5, No. 1, March 1981, pp. 21-34.
- [2] Peters, David A., Boyd, David Doug, and He, Cheng Jian, "A Finite-State Induced-Flow Model for Rotors in Hover and Forward Flight," Journal of the American Helicopter Society, Vol. 34, No. 4, October 1989, pp. 5-17.
- [3] Peters, David A. and Cao, Wenming, "Off-Rotor Induced Flow by a Finite-State Wake Model," 37th AIAA SDM Conference, Salt Lake City, April 15-17, 1996, Paper No. 96-1550.
- [4] Morillo, Jorge and Peters, David A., "Velocity Field above a Rotor Disk by a New Dynamic Inflow Model," Journal of Aircraft, Vol. 39, No. 5, September-October 2002, pp. 731-738.
- [5] Yu, Ke and Peters, David A., "Nonlinear Three-Dimensional State-Space Modeling of Ground Effect with a Dynamic Flow Field," Journal of the American Helicopter Society, Vol. 50, No. 3, July 2005, pp. 259-268.
- [6] Peters, David A., Hsieh, Antonio, and Garcia-Duffy, Cristina, "A Complete Finite-State Inflow Theory from the Potential Flow Equations," Given as the Keynote Lecture and included in the Proceedings of the 3rd International Basic Research Conference on Rotorcraft Technology, Nanjing, China, Oct. 14-16, 2009.
- [7] Fei, Zhongyang and Peters, David A., "A Rigorous Solution for Finite-state Inflow throughout the Flowfield," presented at the 30th AIAA Applied Aerodynamics Conference, New Orleans, Louisiana, June 25-28, 2012.
- [8] Huang, Jianzhe, *Potential-Flow Inflow Model Using Wake Distortion and Contraction*, Ph.D. Thesis, Washington University, May 2015.
- [9] Huang, Jianzhe and Peters, David, "Real-time Solution of Nonlinear Potential Flow Equations for Lifting Rotors," Chinese Journal of Aeronautics, Vol. 30, No. 3, 2017, pp. 871-880.